## Supplementary materials

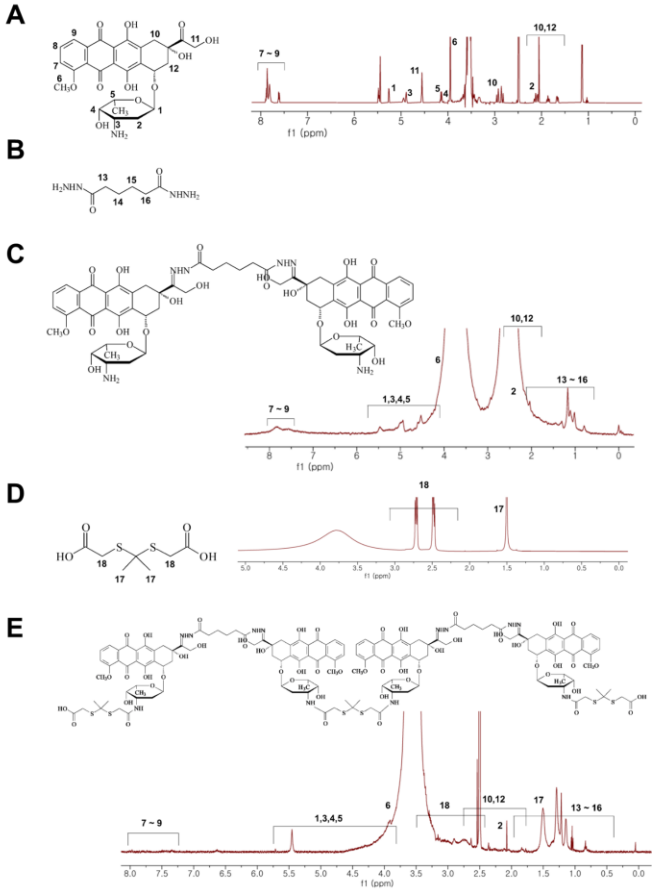


**Figure S1. Chemical structure and $^{1}$H NMR spectra.** To synthesize the PPDHA block copolymer, a DOX tetramer was synthesized and conjugated to PEG and HA. **A**. Doxorubicin (DOX); **B**. Adipic acid dihydrazide (ADH); **C**. DOX dimer ; **D**. Thioketal dicarboxylic acid (ThdCOOH); **E**. DOX tetramer.

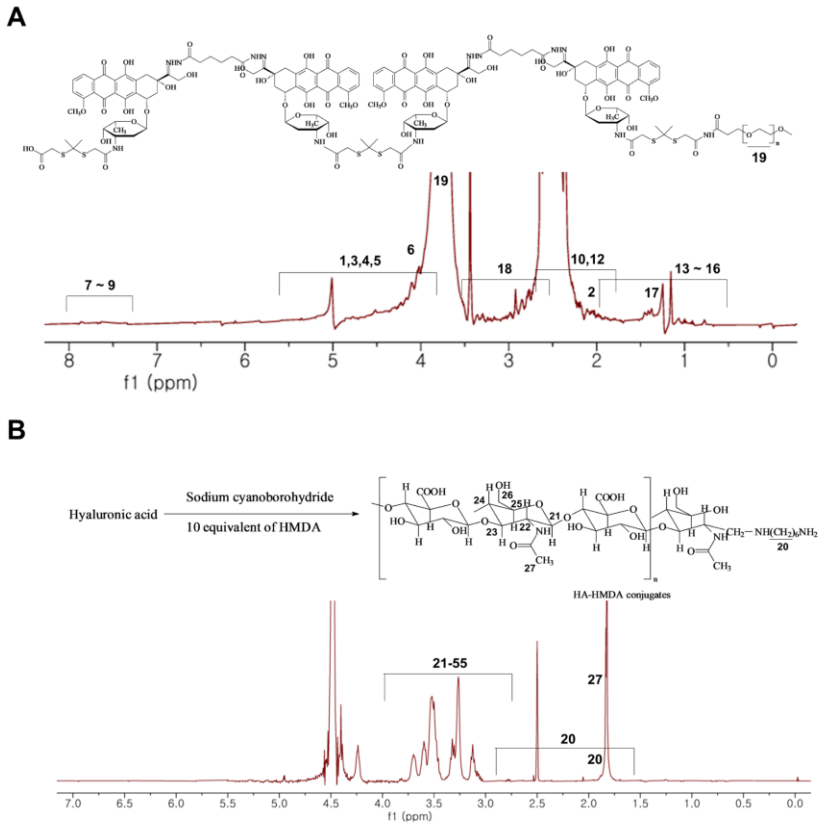


**Figure S2. Synthesis scheme and $^{1}$H NMR spectra of PEG-*b*-DOX tetramer (PPD) and HA-HMDA conjugates. A.** PEG-*b*-DOX tetramer (PPD); **B**. HA-HMDA conjugates**.** To synthesize the PPDHA block copolymer, a DOX tetramer was synthesized and conjugated to PEG and HA as shown in Figure 1a.

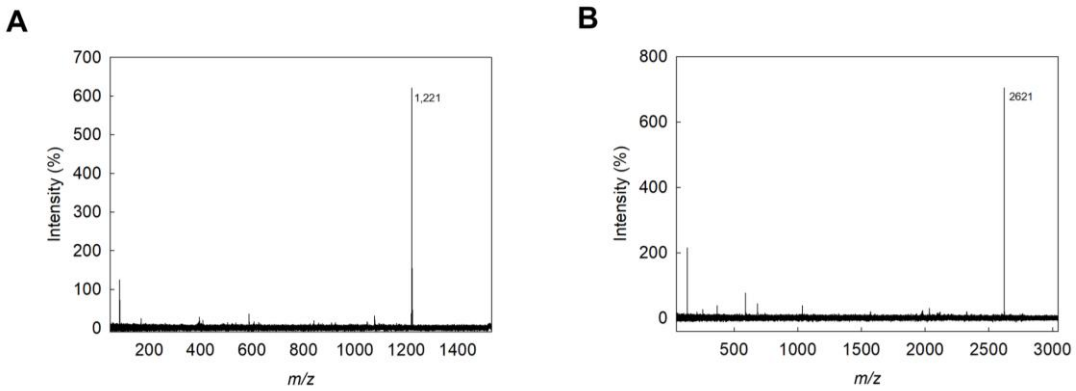


**Figure S3. Molecular weight measurement by HR-TOF mass spectrometry. A.** DOX dimer; **B.** DOX tetramer. HR-TOF was employed to estimate the molecular weight of the DOX dimer and tetramer. Theoretical M.W. of DOX dimer and DOX tetramer were estimated as 1,225 g/mol and 2,638 g/mol, respectively.

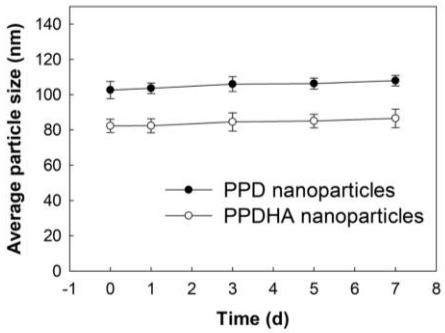


**Figure S4. Stability of PPD and PPDHA nanoparticles in aqueous solution.** PPD or PPDHA nanoparticles in deionized water (4 mg/ml) were stored in refrigerator at 4ºC and then particle size was measured. Particle sizes were expressed as average±S.D. from three different measurements.

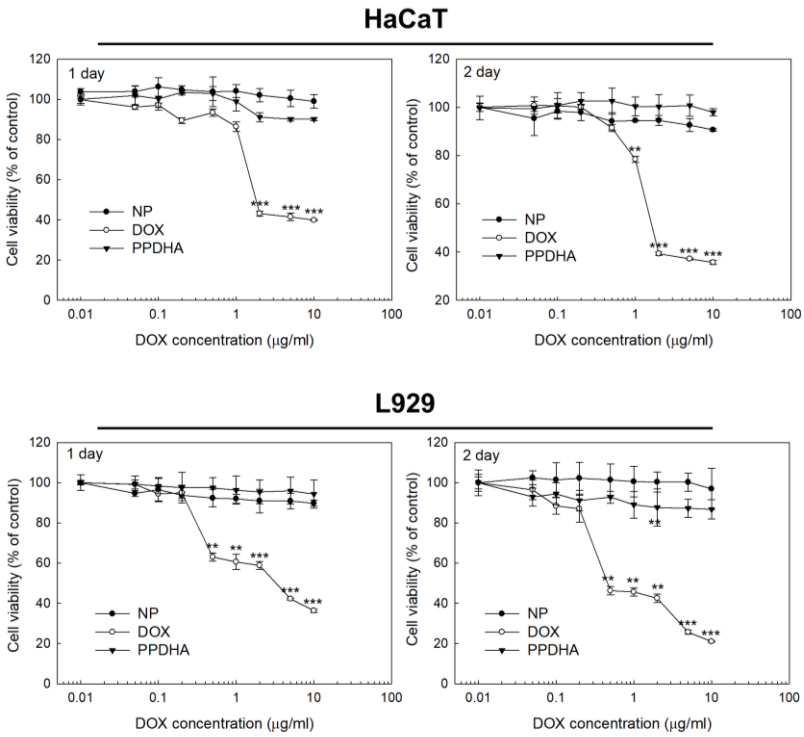


**Figure S5. Cytotoxicity effects of PPDHA in HaCaT and L929 cells.** Empty nanoparticle (NP), DOX and PPDHA (0.01–10 μg/ml) were exposed to HaCaT and L929 cells for 1 day or 2 days and then cell viability was evaluated using the MTT assay. The significance is as follows ** $p < 0.01$, *** $p < 0.001$ compared with the control group.

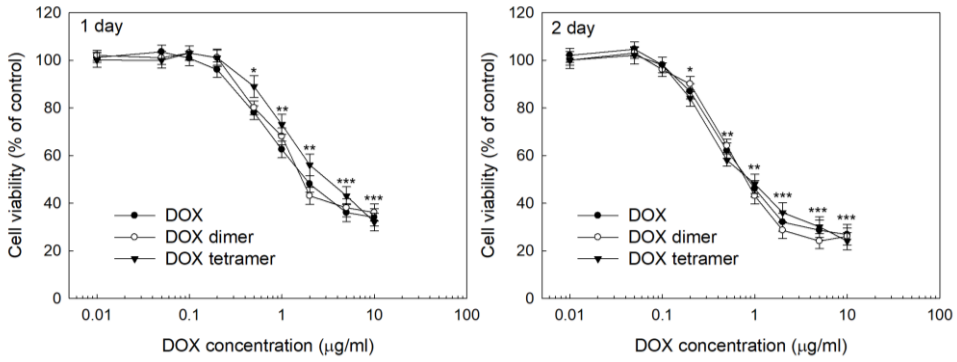


**Figure S6. Cytotoxicity effects of DOX, DOX dimer and tetramer.** DOX, DOX dimer and DOXtetramer (0.01–10 μg/ml) were exposed to MDA-MB-231 cells for 1 day or 2 days and then cell viability was evaluated using the MTT assay. The significance is as follows *p<0.05, ** p < 0.01, *** p < 0.001 compared with the control group

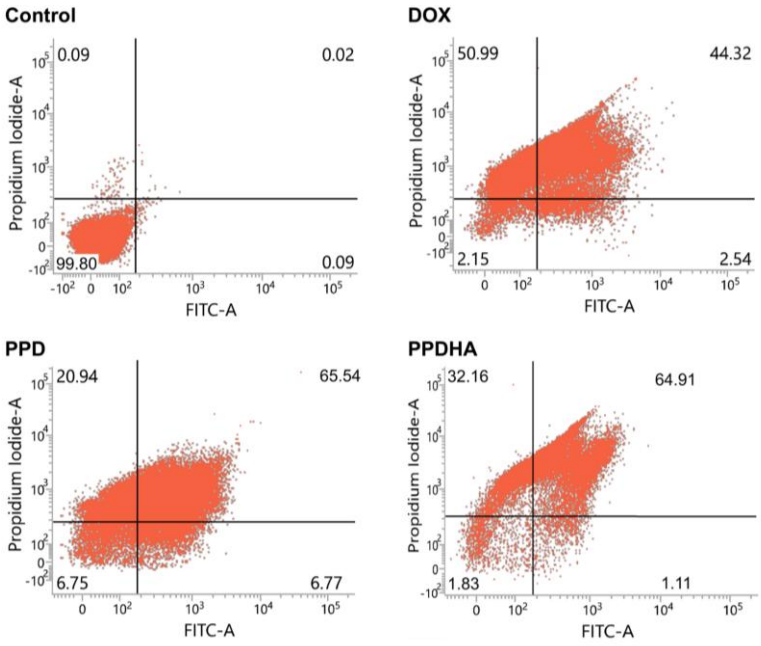


**Figure S7. Apoptosis-inducing effects of PPD and PPDHA Nanoparticles.** MDA-MB-231 cells were stained with FITC-annexin V and PI after 1 d of treatment with DOX, PPD and PPDHA nanoparticles (5μg/ml). The apoptosis rate was detected using a flow cytometer.

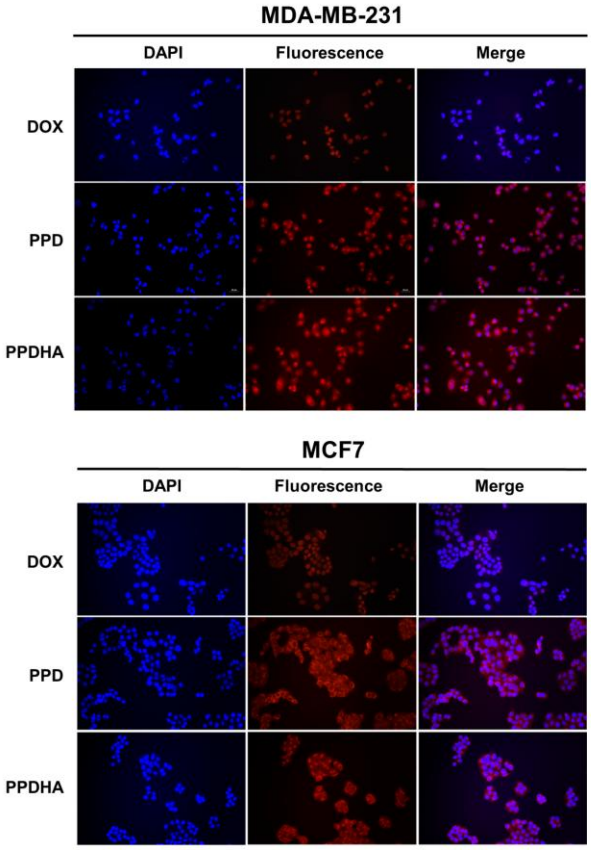


**Figure S8. Intracellular uptake of PPD and PPDHA nanoparticles against MDA-MB-231 cells and MCF7 cells.** MDA-MB-231 and MCF7 cells were incubated with PPD and PPDHA nanoparticles for 2 h to assess intracellular uptake. Following fixation and DAPI staining, intracellular localization of PPD and PPDHA nanoparticles was visualized using fluorescence microscopy.

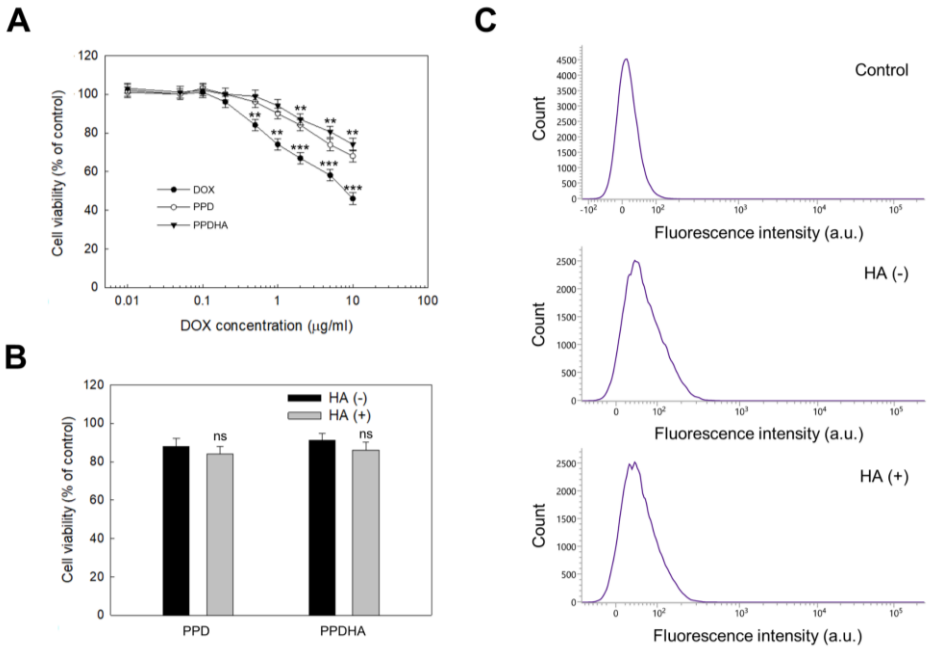


**Figure S9. Cytotoxicity and CD44 receptor blocking effects of PPD and PPDHA on NIH3T3 cells. A**. Cytotoxicity of PPD or PPDHA nanoparticles (0.01–10 μg/ml) against NIH3T3 cells using the MTT assay. **B**. Effect of CD44 receptor blocking on cytotoxicity of PPDHA or PPD nanoparticles (as a DOX, 10 μg/mL) against NIH3T3 cells. Before nanoparticle addition, free HA (100 μg/mL) was added for 1 h to block CD44 receptors of NIH3T3 cells. Then, nanoparticles were exposed to cells for 6 h and then replaced with fresh media followed by further incubation of NIH3T3 cells for 18 h. **C**. Flow cytometer analysis of NIH3T3 cells. Intracellular uptake of PPDHA NPs against NIH3T3 cell was confirmed using flow cytometry. The significance is as follows *p<0.05, ** p < 0.01, *** p < 0.001 compared with the control group. ns, not significant.